Synthetic Metals 222 (2016) 255–266

Contents lists available at ScienceDirect

Synthetic Metals

journal homepage: www.elsevier.com/locate/synmet

# Preparation of polyaniline-coated polyacrylonitrile fiber mats and their application to Cr(VI) removal

Jianyu Ren[a], Xiongyi Huang[b], Ning Wang[a,*], Kezhen Lu[a], Xingxiang Zhang[a], Wei Li[a], Dongqin Liu[c]

[a] Tianjin Municipal Key Lab of Advanced Energy Storage Material and Devices, School of Material Science and Engineering, Tianjin Polytechnic University, Tianjin, 300387, China
[b] Institute of Plasma Physics, Chinese Academy of Science, Anhui, Hefei, 230031, China
[c] Xinxiang Bailu Investment Group Co., Ltd., Henan, Xinxiang, 453011, China

ARTICLE INFO

*Article history:*
Received 6 July 2016
Received in revised form 18 October 2016
Accepted 25 October 2016
Available online 5 November 2016

*Keywords:*
Polyaniline
Polyacrylonitrile
Nanofiber mat
Solution blowing
Hexavalent chromium

ABSTRACT

A composite nanofibers mat containing polyacrylonitrile (PAN) as core and polyaniline (PANI) as sheath had been successfully prepared via solution spinning followed by in situ polymerization, and its hexavalent chromium (Cr(VI)) removal potential was investigated. By altering the processing parameters, bead-free and uniform PAN nanofibers with average diameter of 469 nm could be obtained. The morphological evolution of the PANI/PAN composite fiber mats could be controlled through regulating the molar ratio of oxidant to monomer. The PANI/PAN composite fiber mats presented a superior Cr(VI) adsorption performance. Moreover, the factors affecting the performance of Cr(VI) removal from the aqueous solutions were investigated systematically. The experimental data were fitted to various kinetic models and isothermal adsorption, and the thermodynamic parameters of adsorption process were calculated as well. The PANI/PAN adsorbents were also proven to have good recycling capability, and the mechanism of adsorption and regeneration was investigated in detail.



## 1. Introduction

With the rapid development of economy, environmental pollution is becoming more and more serious, especially the heavy metal ions waste water pollution. Hexavalent chromium is one of the most toxic pollutants in industrial wastewater. In aqueous environment, chromium mainly exists in the two forms of hexavalent Cr(VI) and trivalent Cr(III). The Cr(III) is an essential trace elements of human body, while the Cr(VI) is very toxic and carcinogenic to human body [1,2]. The World Health Organization has recommended that the maximum allowable concentration of Cr(VI) in inland surface water is 0.1 mg/L, and in drinking water is 0.05 mg/L. Thus, it is urgent to explore simple and effective removal method of Cr(VI). Usually chromium-containing wastewater treatment techniques include membrane separation [3], electro-reduction [4], ion exchange [5] and adsorption, [6,7] etc. Among these methods, adsorption technique is widely studied and used owing to its ease of operation, good adsorption capacity and sustainable use of regeneration absorbent. There are many materials used for Cr(VI) removal, such as active carbon [8], agriculture waste [9], metal oxide nanoparticles [10] and polymers [11], etc. Especially with the development of nanotechnology, the nano adsorbent material with great surface area and high porosity has been constantly developed. Compared with traditional adsorbents, nano adsorbent material has higher adsorption efficiency due to its large surface area and more active adsorption sites, etc.

That conductive polymers used for the Cr(VI) removal has already been reported [11–13]. PANI, as an important conductive polymer, has wide potential applications in rechargeable batteries, antistatic coating, biosensors, and adsorption of heavy metal ions because of its ease of preparation, excellent environmental stability, high electrical conductivity and reversible redox behavior [14]. In general, there are three idealized oxidation states of PANI based on the ratio of the amine group and imine group [15]. Leucoemeraldine (LB), emeraldine (EB), and pernigraniline (PB) correspond to the reduced, doped, and oxidized states of PANI, respectively. The amine and imine functional groups in its chain can chelate metal ions and also can absorb anionic metal species through hydrogen bonding or electrostatic [16]. Moreover, PANI is

* Corresponding author.
*E-mail address:* wangntjpu@hotmail.com (N. Wang).

http://dx.doi.org/10.1016/j.synthmet.2016.10.027
0379-6779/

characterized by good solvent resistance and high thermal stability, which makes PANI suitable for various complex environments [11,12]. In previous reports, PANI powders exhibited the high-efficiency for Cr(VI) removal due to its large surface area and numerous active adsorption sites [17–19]. However, it is difficult to recycle the PANI powders after treatment due to its small particle size. It is an effective solution for the recycle to coat PANI on the surface of other easily separated matrix materials (such as chitosan [13], magnetite nanoparticles [20] and fibers [16], etc.). These PANI composites present good performance for the Cr(VI) removal. Polymer nanofiber has received considerable attentions for applications on heavy metals adsorption, due to its technical advantages such as high porosity, great surface area, ease separation from solution [21,22]. However, the adsorption capacity of polymer nanofiber is so small that it would take long time to reach the adsorption equilibrium. Thus, the coating of PANI on polymer nanofiber could make full use of the advantages of PANI and polymer nanofiber. These composites with good adsorption capacity are easy to recycle [23].

As a new fabrication method for nanofibers and microfibers, solution blowing has recently attracted significant attention [24,25]. It combines the superiority of electro spinning in fabricating fibers with diameters from hundreds of nanometers up to a few micrometers and the capability of melt blowing in preparing microfibers on a commercial production scale. In this paper, PAN nanofibers mat (obtained by solution blowing) was used as the base material to obtain PANI/PAN core/shell structure nanofiber. This method is simple and easy to control. The prepared PANI/PAN composites not only kept the original performance of PANI but also could retain the physical and mechanical properties of base fiber material. The composites have potential applications in batteries, electromagnetic shielding, antistatic material, adsorption of heavy metal ions and other fields. The preparation process of PANI/PAN composites was discussed, and the Cr(VI) adsorption properties of PANI/PAN composites was investigated in detail. Besides, the recycling and regeneration of PANI/PAN composites was also studied.

## 2. Experimental

### 2.1. Materials and analytical method

ANI (Tianjin GuangFu Chemical Co., China) was distilled under reduced pressure. PAN was provided by Aladdin. Ammonium persulfate (APS) was provided by Tianjin GuangFu science and technology development Co., China. DBSA was provided by Tianjin Letai Chemical engineering Co., China. Potassium dichromate ($K_2Cr_2O_7$) and 1, 5-diphenylcarbazide (DPC) were purchased from Heowns Biochem Technologies. LLC. Tianjin. Phosphoric acid ($H_3PO_4$, 85 wt%) and sulfuric acid ($H_2SO_4$, 98 wt%) was obtained from Tianjin JiangTian Chemical Technology Co., China. All solutions were prepared in deionized water. The other reagents were in analytical grade.

### 2.2. Solution blow spinning of PAN nanofibers mat

The process for solution blow spinning of PAN nanofibers mat was as follows: PAN was dissolved in 50 g DMF and stirred at 60 °C for 12 h to obtain homogeneous solution with a concentration of 12 wt%. The PAN solution was spun into nanofibers mat using a

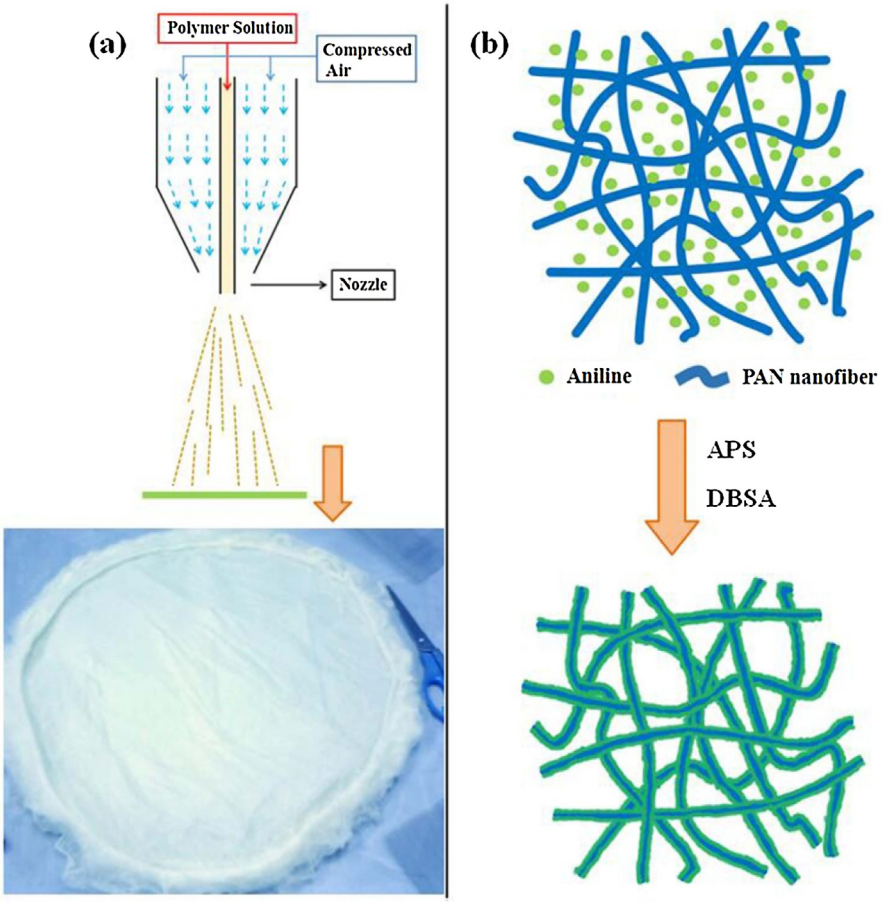


**Fig. 1.** Schemes of the PAN nanofibers preparation (a) and the PAN/PANI composites preparation (b).

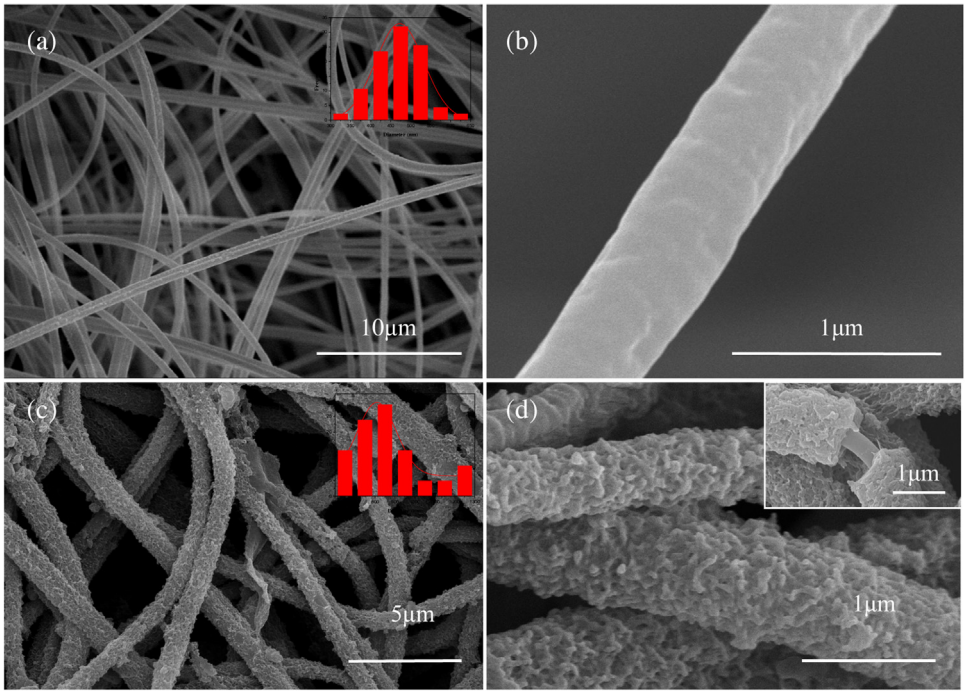


**Fig. 2.** (a) SEM images of PAN nanofibers (large scale); (b) SEM images of PAN nanofibers (small scale); (c) PANI/PAN composite fibers (large scale); (d) PANI/PAN composite fibers (small scale).

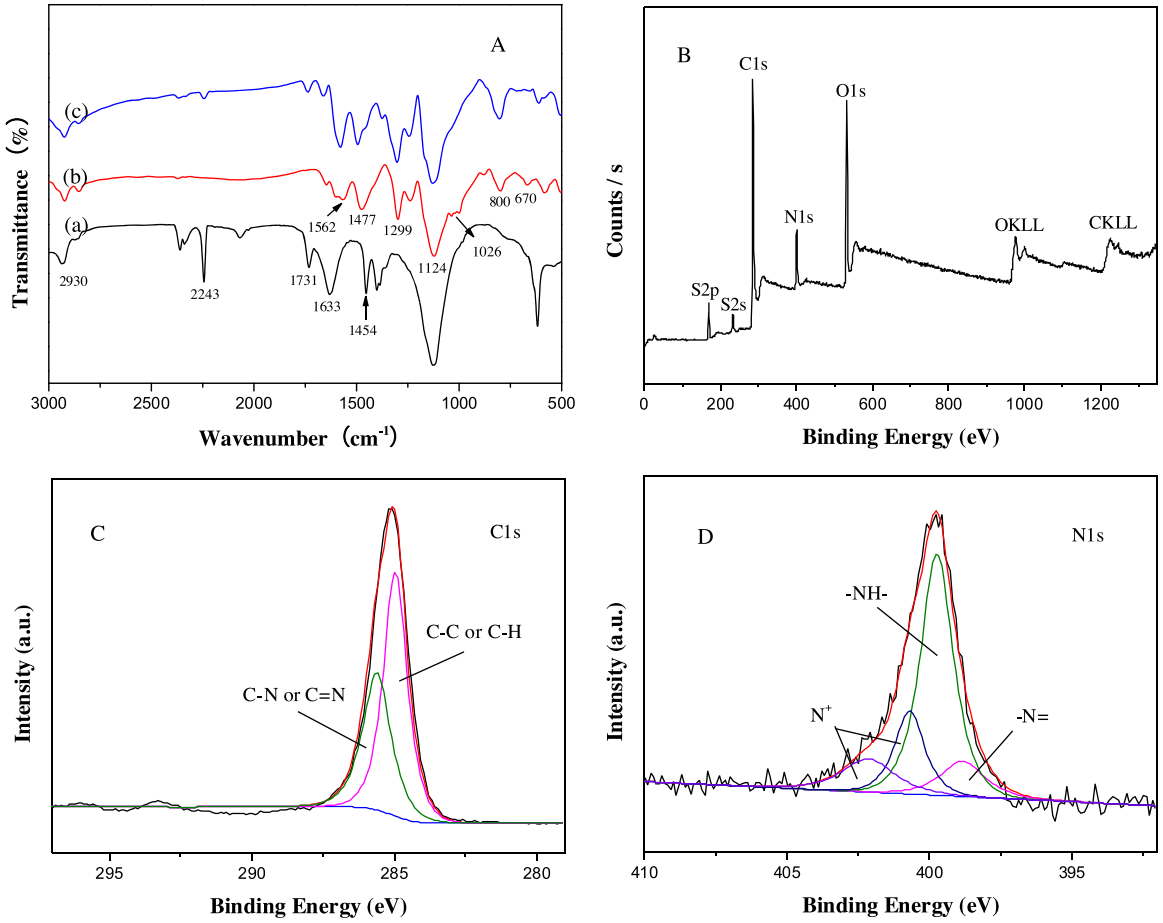


**Fig. 3.** (A) FT-IR spectra of (a) pure PAN nanofibers mat, (b) DBSA doped PANI, and (c) DBSA-PANI/PAN composites; (B) XPS wide scan and (C) C1s, (D) N1s spectra of DBSA doped PANI/PAN.

solution blow spinning apparatus. It consisted of a high velocity compressed air supply, a pump, a spinning die, a spinning cabinet and a collector. In the spinning process, we used the cylindrical steel nozzle with diameter of 0.5 mm as the spinning die. The spinning solution was supplied to the nozzle and formed a solution stream by the high velocity airflow. Then, the solution was blown and attenuated into ultrafine fibers, accompanied with the evaporation of the solvent. The collecting distance was set as 800 mm which was constant in all the experiments. The process for preparation of PAN nanofibers mat is illustrated in Fig. 1(a). The thickness of the nanofibers mat is about 100 μm.

### 2.3. In situ deposition of PANI on PAN nanofibers mat

The PANI/PAN core/shell nanofibers mat was prepared by in situ polymerization of PANI on the surface of PAN nanofibers mat. 10.28 g DBSA was added into 200 mL ethanol/water solution. The ratio of ethanol and water was 20:50 (v/v). PAN nanofibers mat (about 5 × 5 cm) was immersed into the DBSA ethanol/water solution. ANI was added into the solution, and then stirred for 30 min. APS solution was added dropwise into the above system. The reaction was carried out at 0 °C. The mole ratio of aniline/DBSA/APS was 1/1.5/1.5. The reaction products were filtrated and washed successively with ethanol and deionized water until the filtrate become colorless, and then dried at 60 °C for 12 h in vacuum to obtain PANI/PAN composites. The process for preparation of PANI/PAN composites is shown schematically in Fig. 1(b).

### 2.4. Cr(VI) adsorption experiments

The adsorption experiments were carried out with 25 mL of Cr (VI) solution using 10 mg of PANI/PAN nanofibers mat placed in a temperature controlled thermostatic oscillator operated at 100 rpm for 6 h. The pH of the solution was adjusted by 0.1 M NaOH and 0.1 M $H_2SO_4$. The concentration of Cr(VI) was analyzed by spectrophotometer using 1,5-diphenylcarbazide (DPC) as the complexing agent at a wavelength of 540 nm (GB 7467-87) [8,26].

The removal percentage ($R\%$) of Cr(VI) was calculated by the following equation:

$$R\% = \frac{C_o - C_e}{C_o} \times 100\% \quad (1)$$

where $C_o$ is the initial concentration of Cr(VI) in solution (mg/L) and $C_e$ is the equilibrium concentration (mg/L).

The adsorption isotherms were established by batch adsorption experiments. 40 mg PANI/PAN fibers mat was immersed into 100 mL Cr(VI) solutions with different initial concentration. The initial pH of Cr(VI) solutions was adjusted to 1.0 by using 0.1 M $H_2SO_4$ and 0.1 M NaOH. The adsorption was carried out at three different temperatures (i.e. 25, 40 and 55 °C) with constant shaking, and then kept for 12 h to establish adsorption equilibrium. The equilibrium adsorption capacity was determined using the following equation:

$$q_e = \frac{C_o - C_e}{m} V \quad (2)$$

where $C_o$ is the initial concentration of Cr(VI) in solution (mg/L), $C_e$ is the equilibrium concentration (mg/L), $q_e$ is the equilibrium adsorption capacity (mg/L), $m$ is the mass of adsorbent (g), and $V$ is the volume of solution (L), respectively.

For the kinetic adsorption experiments, 40 mg of PANI/PAN nanofibers mat was immersed into 100 mL Cr(VI) solutions with different initial concentration at 25 °C. The initial pH of Cr(VI) solution is 1.0, and the solution was shaken in a thermostatic shaker bath during the process. An appropriate amount of the solution were taken at different time and tested. The adsorption capacity was calculated by the following equation:

$$q_t = \frac{C_o - C_t}{m} V \quad (3)$$

where $q_t$ is the adsorption capacity at time t (mg/g), $C_o$ is the initial concentration of Cr(VI) in solution (mg/L), $C_t$ is the Cr(VI) concentration at time t (mg/L), $m$ is the mass of the adsorbent (g), and $V$ is the volume of solution (L), respectively.

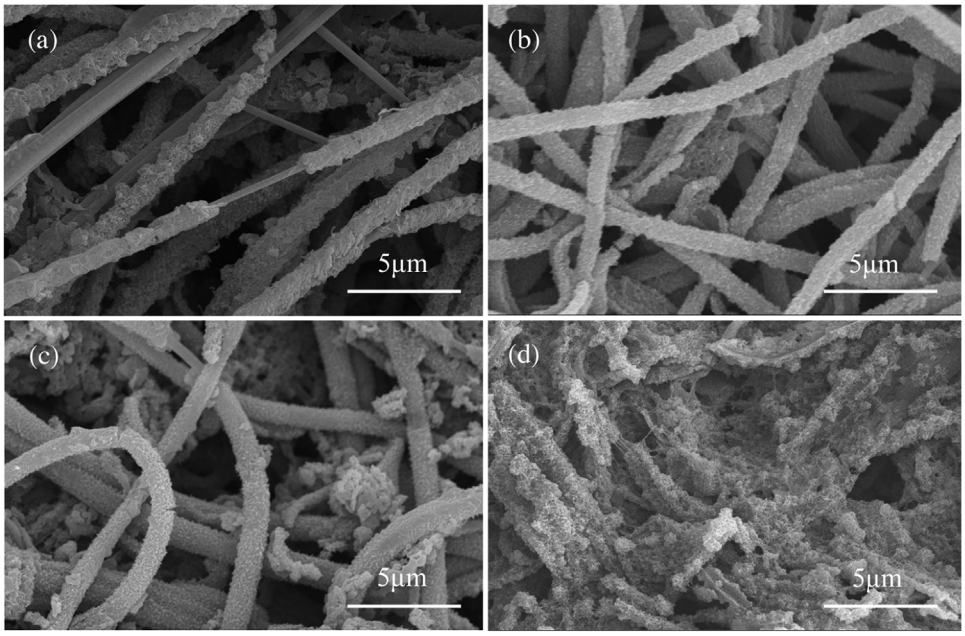


**Fig. 4.** SEM images of PANI/PAN composite obtained with different [APS]/[aniline] ratio: (a) 1:1; (b) 1.5:1; (c) 2:1; (d) 3:1.

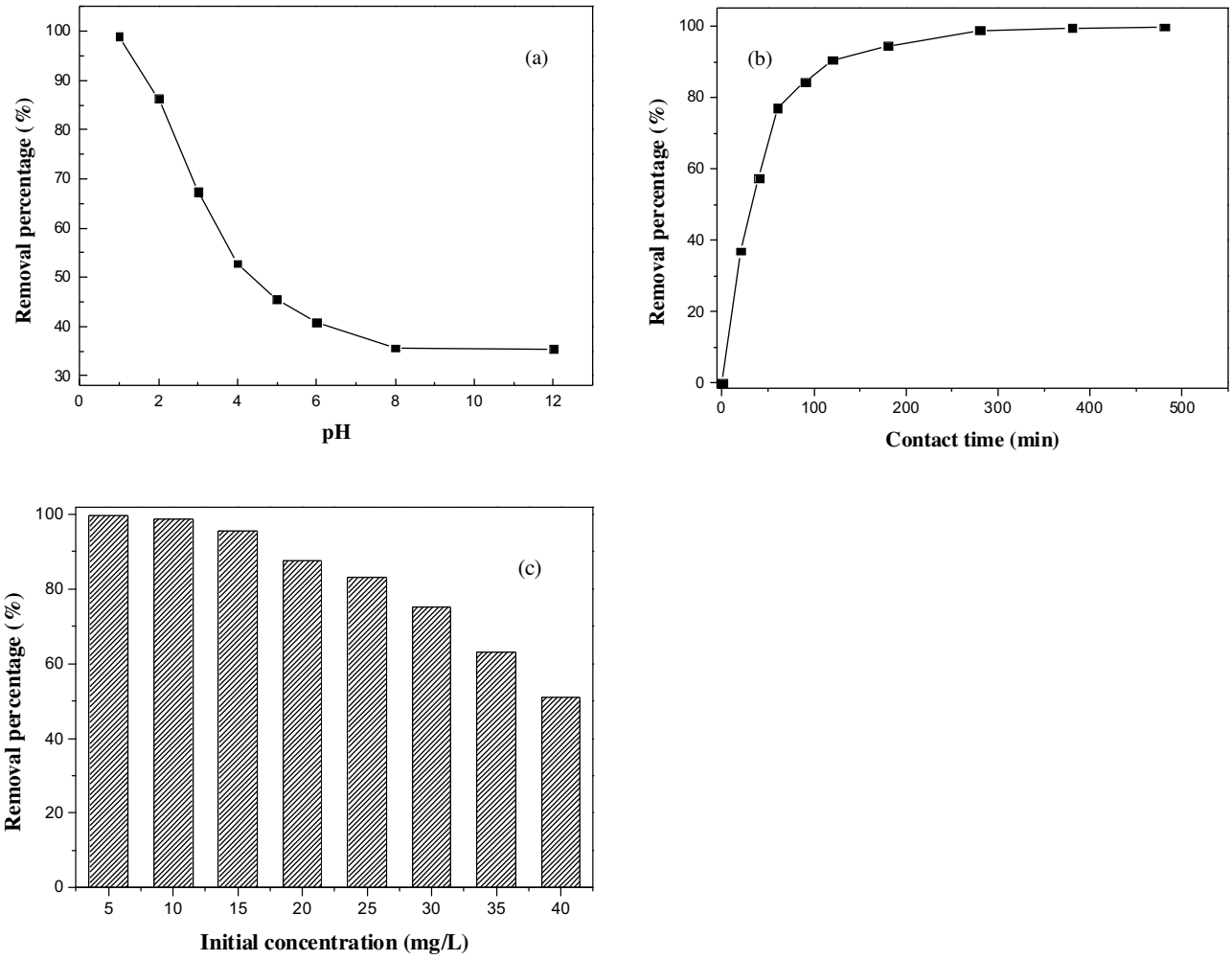


**Fig. 5.** Effect of pH (a), contact time (b) and initial Cr(VI) concentration (c) on the removal of Cr(VI) by the PANI/PAN fibers mat.

### 2.5. Regeneration experiment

For regeneration studies, the PANI/PAN fibers mat were used to treat 25 mL Cr(VI) solution (5.0 mg/L) for 6 h at 25 °C, and then were taken out and regenerated by immersing into 25 mL HCl solution (0.1 M) for 30 min [27,28]. The Cr adsorbed on the PANI/PAN was released in the desorption solution. The PANI/PAN nanofibers mat were then washed with deionized water until pH reached 7. The regenerated PANI/PAN were then used to treat 25 mL Cr(VI) solution (5.0 mg/L) again. The adsorption–desorption processes

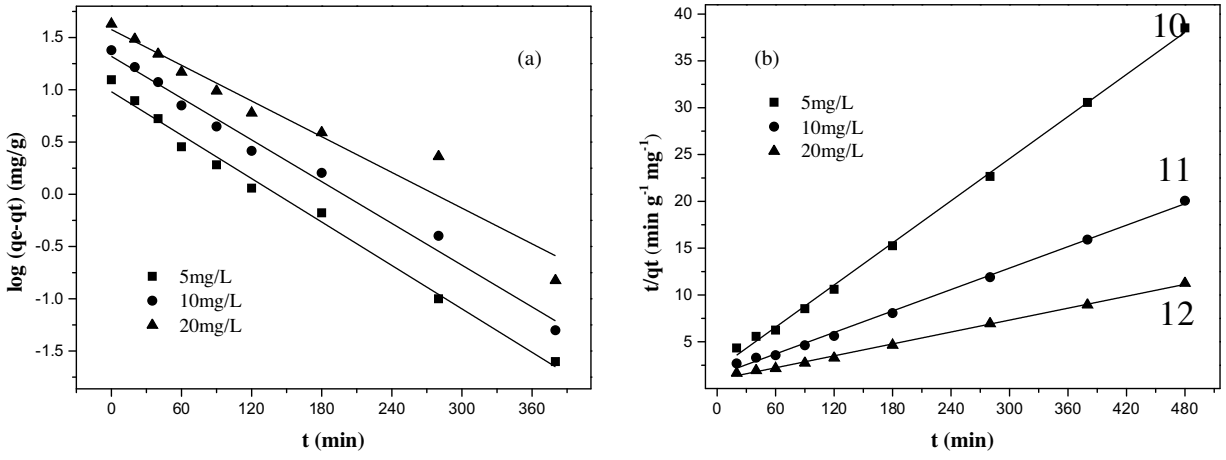


**Fig. 6.** Pseudo-first-order kinetic model (a), pseudo-second-order kinetic model (b) for adsorption of Cr(VI) onto PANI/PAN fibers mat.

**Table 1**
Kinetics parameters for Cr(VI) adsorption onto PAN/PANI nanofibers mat.

| $C_0$(mg $L^{-1}$) | experimental | pseudo-first-order model | | | pseudo-second-order model | | |
|---|---|---|---|---|---|---|---|
| | $q_e$(mg $g^{-1}$) | $K_1$ | $q_{e1}$ | $R^2$ | $K_2$ | $q_{e2}$ | $R^2$ |
| 5 | 12.46 | 0.01596 | 9.58 | 0.99018 | $2.72 \times 10^{-3}$ | 13.34 | 0.99833 |
| 10 | 23.92 | 0.01534 | 20.90 | 0.98781 | $1.03 \times 10^{-3}$ | 26.18 | 0.99703 |
| 20 | 42.60 | 0.01313 | 37.71 | 0.94191 | $0.47 \times 10^{-3}$ | 47.14 | 0.99753 |

$q_e$: equilibrium adsorption capacity from experiments. $q_{e1}$, $q_{e2}$: equilibrium adsorption capacity calculated from kinetic models.

were conducted for 5 times. The Cr(VI) removal efficiency by the generated PANI/PAN was determined each time.

### 2.6. Characterizations

The surface morphology was characterized by field emission scanning electron microscope (FE-SEM, S4800 Hitachi, Japan). The functional groups were characterized by FTIR spectroscope (Bruker Vector 22, Germany) which was recorded with a resolution of 4 $cm^{-1}$ in the transmission mode. Raman spectra excited with a HeNe 633 nm laser were collected on a Renishaw inVia Reflex Raman microscope. XPS measurements were performed by using K-alpha, ThermoFisher, equipped with an Al Kα radiation source (1486.6 eV). The XPS spectra data was accomplished with the software XPSPEAK4.1. The diameters of the fibers and its distributions were analyzed with an image analyzer (Image-Pro Plus, Media Cybernetics). Viscosity of spinning solutions was measured at room temperature using a NDJ-79 rotary viscometer (Shanghai Chang ji Geological Instruments Co, Ltd., Shanghai, China). Each data shown here was the mean value of the measurement from at least three samples.

## 3. Results and discussion

### 3.1. Characteristics of PANI/PAN composites

As shown in Fig. 1(a), PAN nanofibers mat with diameter of 350 mm could be obtained in this experiment. The PAN nanofibers

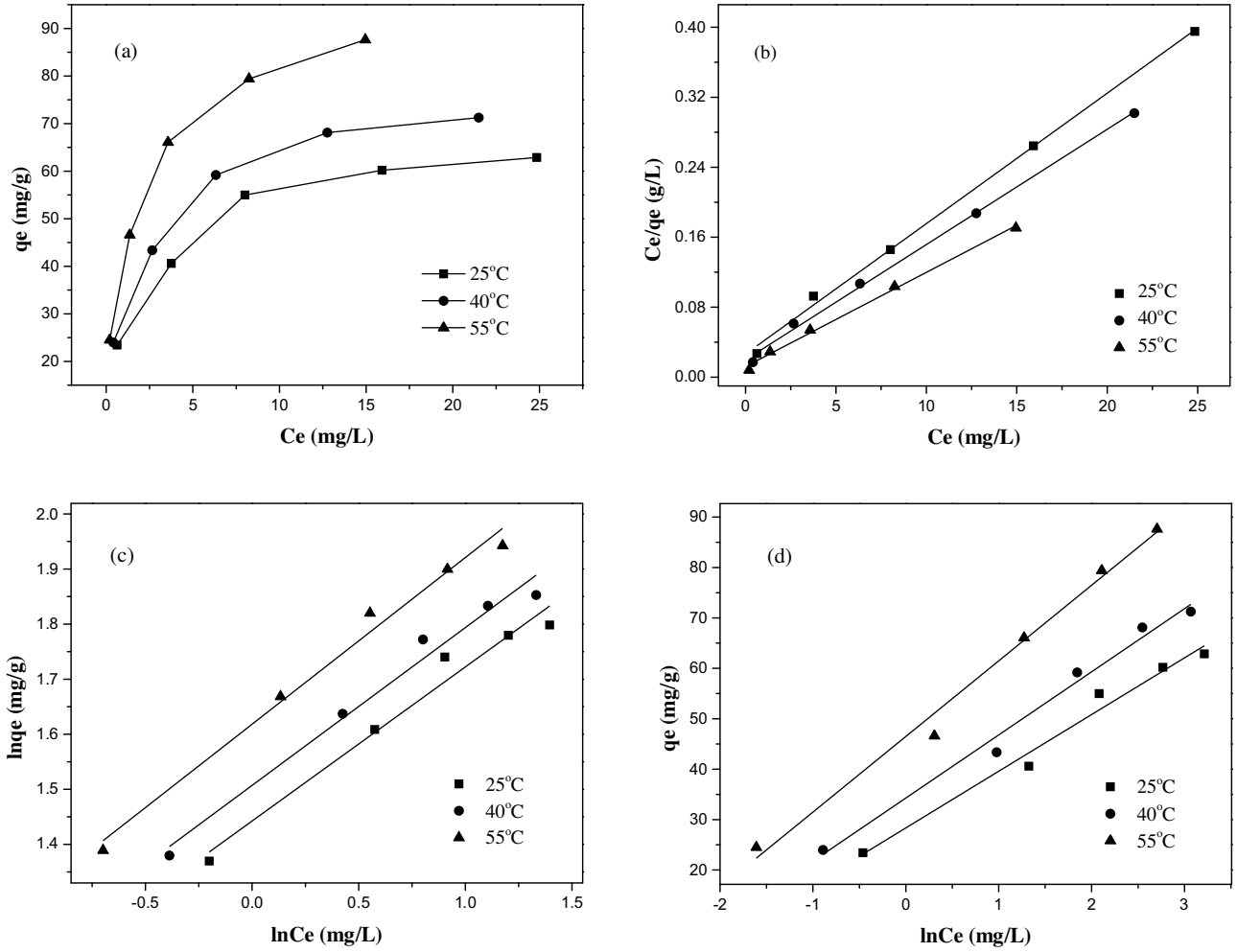


**Fig. 7.** (a) The plot of adsorption capacity against initial Cr(VI) concentration; (b) Langmuir adsorption isotherm, Freundlich adsorption isotherm (c) and Temkin isotherm (d) for Cr(VI) ions adsorption on the PANI/PAN nanofibers mat.

**Table 2**
Parameters of the Langmuir, Freundlich, and Temkin isotherm models.

| Temperature(°C) | Langmuir model | | | Freundlich model | | | Temkin model | | |
|---|---|---|---|---|---|---|---|---|---|
| | $q_m$(mg/g) | b(L/mg) | $R^2$ | $K_f$(mg/g) | n | $R^2$ | A(L/g) | B(KJ/mol) | $R^2$ |
| 25 | 67.07 | 0.56 | 0.997 | 27.70 | 3.57 | 0.963 | 28.35 | 11.24 | 0.974 |
| 40 | 75.93 | 0.66 | 0.997 | 32.15 | 3.49 | 0.974 | 34.27 | 12.52 | 0.982 |
| 55 | 92.85 | 0.89 | 0.996 | 41.52 | 3.30 | 0.982 | 46.49 | 15.00 | 0.986 |

mat was composed of the entangled individual fibers. From the SEM images (Fig. 2(a) and (b)), it could be found that the average diameter of the nanofibers was 469 nm and the surface of nanofibers was smooth and compact. Moreover, the nanofibers were three-dimensional network structures due to the effect of the turbulent flow in the gas flow field. This feature results in entangled nanofibers forming mats with high porosity which favor the improvement of the dispersion of PANI.

Fig. 2(c) and (d) shows the SEM microstructures of the PANI/PAN core/sheath nanofibers. Compared with the pure PAN nanofibers (Fig. 2(a) and (b)), the surface of PANI/PAN composites became rougher, and the average diameter increased to about 400 nm. Moreover, the PAN/PANI nanofibers showed a similar network structure. The results indicate that PANI was successfully coated on the surface of PAN nanofibers. And it could be observed that PANI formed a complete layer. And the core/sheath structure can be found from Fig. 2(d). The above results indicate that the lacunaris PAN nanofibers mat acted as a template with network structure during the polymerization of aniline. Compared with traditional adsorbents, the PANI/PAN nanofibers mat has higher adsorption capacity due to its large surface area and more active adsorption sites.

The FTIR spectra of PAN, DBSA doped PANI and DBSA-PANI/PAN composite are shown in Fig. 3A. For PAN, the band at 2243 $cm^{-1}$ is originated from the —C≡N— group stretching which turned weaken in the spectrum of PANI/PAN composites, the band at 1731 $cm^{-1}$ is due to free carbonyl group absorption, the bands at 2930 and 1454 $cm^{-1}$ are assigned to the stretching vibration and bending vibration of methylene (-$CH_2$-). The positions of these peaks in PANI/PAN composites shift to slightly lower values due to the presence of PANI on the PAN surface. The DBSA doped PANI FTIR spectra showed that the absorption peaks at 1562 and 1477 $cm^{-1}$ correspond to the C=C stretching vibration of N = Q = N (Q = quinoid ring) and N–B–N (B = benzene ring) respectively [17]. The absorption peaks of 1299 and 1124 $cm^{-1}$ correspond to C—N and C—H stretching vibration in the benzene ring. Absorption peak at 800 $cm^{-1}$ correspond to C—H in-plane bending vibration of the benzene rings. From the DBSA O = S=O stretching vibration peak appeared at the 1299 $cm^{-1}$, S–O stretching vibration peak appeared at the 670 $cm^{-1}$, between DBSA and PANI chain formed $NH^{+}\cdots SO_3^{-}$ absorption peak appeared at 1026 $cm^{-1}$ [29]. The characteristic peak of PAN and PANI could be detected in Fig. 3A(c) (PANI/PAN). Hence, these FTIR spectra reveals that PANI was well doped, and PANI was coated on the surface of PAN nanofibers, as illustrated by SEM images.

Fig. 3 B, C and D shows the XPS spectra of the synthesized PANI/PAN. In the wide scan spectra of the PANI/PAN (Fig. 3 B), O1s and S2p signals appearing at 530 and 169 eV reveal that PAN are wrapped underneath doped PANI coatings forming core-shell structure in DBSA doped PANI/PAN composites. The C1s peak was deconvoluted into two major components with peaks at 284.9 and 285.6 eV (Fig. 3(C)), which are attributed to C—C or C—H and C—N or C=N, respectively [30]. Fig. 3(D) shows the N1s XPS spectra. The N1 s spectrum was deconvoluted into four major peaks [31] at 398.8 (-N = ), 399.7 (-NH-), 400.7 (-$N^{+}$=) and 402.1 (-$N^{+}$-) eV. Their percentages of total N1 s intensity are 11.3, 57.8, 18.1 and 12.7% for the peaks 398.8, 399.7, 400.7 and 402.1 eV respectively. The protonation degree can be characterized by the proportion of the intensity of these peaks (-$N^{+}$=/(-N = +-$N^{+}$ = ). Thus, the protonation degree of DBSA-PANI was found to be 61.2%. All the above results illuminate that uniform DBSA-PANI layers were successfully coated on the surface of PAN nanofibers, which is consistent with the FT-IR and SEM analysis.

As shown in Fig. 4. When the concentration of oxidant APS increased, the surface morphology of the PANI/PAN was found to be changed. The composites showed a good surface morphology when the [APS]/[aniline] ratio increased to 1.5:1. The succeeding growth of PANI chains on these radical cations made much more aniline monomers polymerize on the PAN nanofibers, and finally formed a closer accumulation [32].

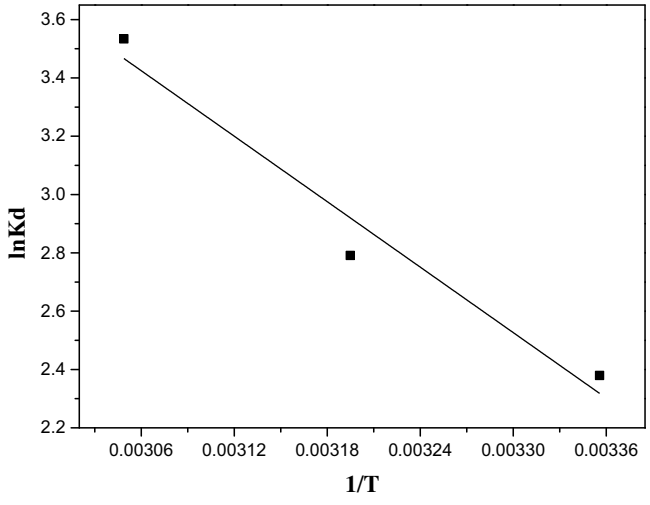


**Fig. 8.** Plot to determine thermodynamic parameters of Cr(VI) adsorption onto PANI/PAN fibers mat.

### 3.2. Cr(VI) removal

#### 3.2.1. pH effect on the adsorption

The initial pH value of solution plays an important role during the Cr(VI) removal process. The Cr(VI) removal percentage by PANI/PAN under different initial pH environment is shown in Fig. 5(a) with a PANI/PAN dose of 10 mg and 25 mL Cr(VI) solution (5 mg/L).

**Table 3**
Thermodynamic parameters for Cr(VI) uptake by the PANI/PAN fibers mat.

| Temperature(°C) | $\Delta G^{o}$ (KJ/mol) | $\Delta H^{o}$ (KJ/mol) | $\Delta S^{o}$ (J/mol/K) |
|---|---|---|---|
| 25 | −5.895 | 31.113 | 123.678 |
| 40 | −7.263 | | |
| 55 | −9.638 | | |

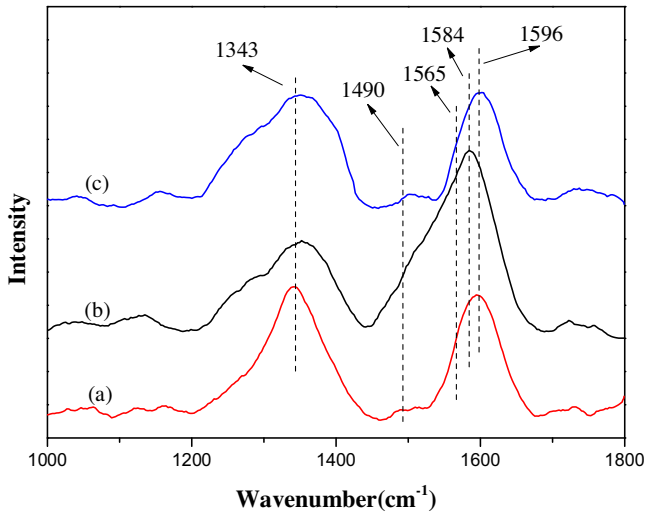


**Fig. 9.** Raman spectra of (a) PANI/PAN, (b) PANI/PAN after treated with Cr(VI) solution and (c) PANI/PAN after regenerated by 0.1 M HCl solution, respectively.

The initial pH of chromium solutions was adjusted from 1 to 12 with NaOH or $H_2SO_4$ solutions. According to Fig. 5a, when the initial pH changed from 1.0 to 12.0, the removal percentage decreased from 98.9% to 35.4%. So it was obvious that the adsorption of Cr(VI) on the PANI/PAN was highly pH dependent. According to the literature [33], the predominant forms of Cr(VI) in aqueous solutions are $HCrO_4^-$ when the pH < 6.8, and the dominant forms is $CrO_4^{2-}$ when the pH > 6.8. The $H_2CrO_4$ concentration is increased when the solution pH < 2.0 [33], which indicates that the PANI/PAN favors the reduction of hydrogen chromate ($HCrO_4^-$ and $H_2CrO_4$). The possible reasons for high Cr (VI) removal by PANI/PAN in acidic solutions is as follows: there is bonding between hydrogen chromate and the amine group of the PANI/PAN [33], the $HCrO_4^-$ with a higher redox potential (1.33 eV) in an acidic solution can be easily reduced to Cr(III) (see Eq. (4)) [11]. However, in alkaline solution, $CrO_4^{2-}$ is the dominant forms. The oxidation ability of $CrO_4^{2-}$ is weaker than that of $HCrO_4^-$ because of the low redox potential (−0.13 V) (see Eq. (5)) [34]. And there are competitive interaction between the hydroxyl ($OH^-$) ions and $CrO_4^{2-}$ ions for the same adsorption active sites on the adsorbent surface [35], which consequently decrease the Cr(VI) removal capacity.

$$HCrO_4^- + 7H^+ + 3e^- \rightarrow Cr(III)\downarrow + 4H_2O \quad E_o = 1.33\ V \tag{4}$$

$$CrO_4^{2-} + 4H_2O + 3e^- \rightarrow Cr(OH)_3 + 5OH^- \quad E_o = -0.13\ V \tag{5}$$

*3.2.2. Contact time effect on the adsorption*

As shown in Fig. 5(b), the effect of contact time on the adsorption was studied from the adsorption experiments. All experiments were carried out three times and a good reproducibility of the procedures was obtained. The PANI/PAN composite could reach at adsorption equilibrium within 6 h when the initial concentration of Cr(VI) was 5.0 mg/L with a pH of 1.0. And the Cr (VI) removal percentage reached a maximum of 99.66%. And there was no further adsorption above 300 min, so the optimal contact time for the adsorption of Cr(VI) (5.0 mg/L) could be determined as 300 min. The results indicate that the PANI/PAN is considered as a suitable adsorbent for removal of Cr(VI) with low concentrations.

*3.2.3. Initial concentration effect on the adsorption*

The effect of initial Cr(VI) concentration on the Cr(VI) removal percentage by PANI/PAN fibers mat was investigated and the results is shown in Fig. 5(c). It was observed that 0.4 g/L PANI/PAN fiber mat could completely remove the Cr(VI) with a concentration below 10.0 mg/L and pH = 1.0. And the removal percentage then decreased with the initial Cr(VI) concentration increased. It was mainly due to the saturation of sorption sites or non-availability of PANI/PAN surface. Moreover, the high redox potential of solution with high Cr(VI) concentration results in the degradation of PANI on the surface of composite mat [36], which might leads to a decreased Cr(VI) removal percentage. However, more than 51% Cr (VI) could be removed by PANI/PAN fibers mat even when the initial Cr(VI) concentration was up to 40 mg/L.

*3.2.4. Adsorption kinetics*

Two common types of kinetic models, namely, the pseudo-first-order [37], and the pseudo-second-order [38], were employed to investigate the adsorption process of Cr(VI) on to PANI/PAN fiber mat. These two kinetic models are used to describe the adsorption of solid/liquid systems, which can be expressed in the linear forms as Eqs. (6) and (7), respectively:

$$\log(q_e - q_t) = \log q_e - \frac{K_1}{2.303}t \tag{6}$$

$$\frac{t}{q_t} = \frac{1}{K_2 q_e^2} + \frac{1}{q_e}t \tag{7}$$

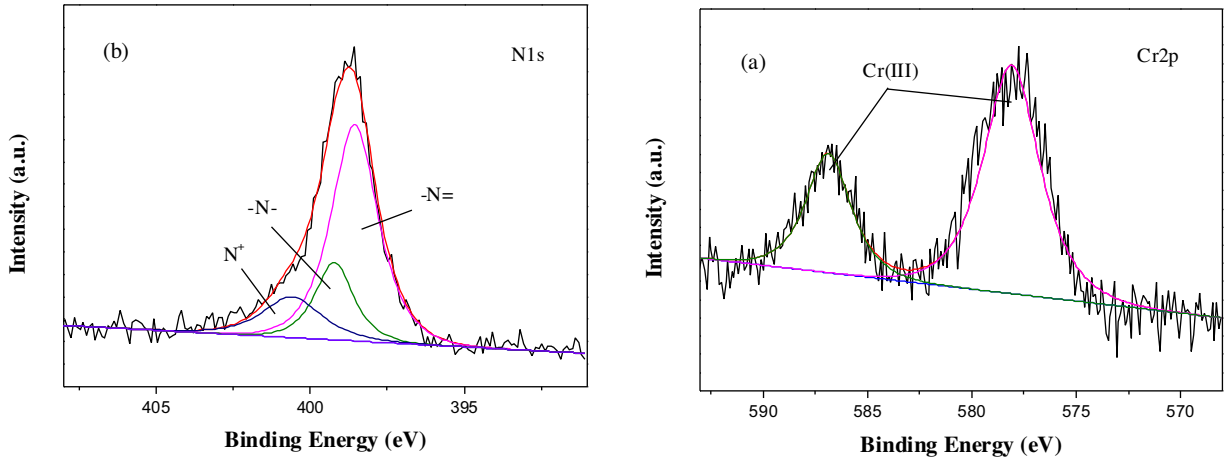


**Fig. 10.** (a) Cr 2p XPS spectra and (b) N1s XPS spectra of the PANI/PAN (10 mg) after treatment with 25.0 mL Cr(VI) solution (5.0 mg/L pH = 1.0) for 6 h at room temperature.

where $K_1$ and $K_2$ are the pseudo first order and second order rate constants, respectively.

The adsorption kinetic plots are shown in Fig. 6 and the obtained kinetic parameters are summarized in Table 1. The values of the correlation coefficients ($R^2$) clearly indicated that the adsorption kinetics closely followed the pseudo-second-order model. The $q_e$ values obtained from pseudo-second-order kinetic model were close to the experimentally observed values. The results indicate that the adsorption kinetics closely followed the pseudo-second-order model.

### 3.2.5. Adsorption isotherms

To investigate the adsorption capacity and thermodynamics of Cr(VI) adsorption by PANI/PAN fibers mat, adsorption isotherms were studied at 25, 35 and 55 °C, respectively, and the results are presented in Fig. 7a. It is obvious that the adsorption capacity increased when the temperature increased, indicating that Cr(VI) removal by the PANI/PAN is an endothermic process in nature.

Langmuir, Freundlich and Temkin isotherm models were widely used to fit the equilibrium data. The three linear isotherm equations are expressed as follows:

$$\text{Langmuir}: \quad \frac{C_e}{q_e} = \frac{C_e}{q_m} b + \frac{C_e}{q_m} \tag{8}$$

$$\text{Freundlich}: \quad \ln q_e = \ln k_F + \frac{1}{n} \ln C_e \tag{9}$$

$$\text{Temkin}: \quad q_e = A + B \ln C_e \tag{10}$$

where $C_e$ are the equilibrium concentrations (mg/L); $q_m$ and $b$ are the Langmuir constants related to the adsorption capacity (mg/g) and the rate of adsorption (L/mg), respectively; $k_F$ and $n$ are the Freundlich isotherm parameters related to adsorption capacity (mg/g) and intensity of adsorption, respectively; $A$ and $B$ are the Temkin isotherm constants.

The linearized Langmuir, Freundlich and Temkin isotherms for the three different temperatures are shown in Fig. 7. And the values of these isotherm parameters are summarized in Table 2. The higher values of correlation coefficient ($R^2$) reveals that the Langmuir model fitted well the isotherm data compared with the other two models, suggesting a monolayer adsorption for the uptake of Cr(VI) on the surface of the PANI/PAN fiber mat. The high adsorption capacity, easy and cost effective synthesis of the PANI/PAN fiber mat further suggests its potential application in industrial wastewater treatment.

### 3.2.6. Thermodynamic investigations

The thermodynamic parameters associated with the adsorption process, standard Gibbs free energy change ($\Delta G^o$), enthalpy change ($\Delta H^o$), and entropy change ($\Delta S^o$) were calculated by the following equations [34]:

$$\ln K_d = \frac{\Delta S^o}{R} + \frac{-\Delta H^o}{RT} \tag{11}$$

$$K_d = \frac{(C_o - C_e)V}{mC_e} \tag{12}$$

$$\Delta G^o = -RT \ln K_d \tag{13}$$

where $m$ is the adsorbent dose (g), $R$ (J/mol/K) is the ideal gas constant, $T$ (K) is the absolute solution temperature and $K_d$ (L/mol) is the thermodynamic equilibrium constant.

The values of $\Delta H^o$ and $\Delta S^o$ were obtained from the slope and intercept of the plot of $\ln K_d$ versus 1/T (shown in Fig. 8). The values of $\Delta G^o$, $\Delta H^o$ and $\Delta S^o$ are summarized in Table 3. From the plot, both the change in entropy ($\Delta S^o$) and the enthalpy ($\Delta H^o$) of adsorption were determined to be 123.678 J/mol/K and 31.113 kJ/mol, respectively. The positive value of $\Delta H^o$ confirms that the adsorption process is endothermic. With an increase in temperature, negative values of change in Gibbs free energy ($\Delta G^o$) are obtained which indicate the spontaneity of the adsorption process. The positive value of $\Delta S^o$ indicates the increase in randomness at the PANI/PAN fiber-solution interface due to the release of dodecylbenzene sulfonate anion ions, which are present on the surface of the adsorbent.

### 3.2.7. Cr(VI) removal mechanisms

The Cr(VI) removal mechanism by PANI/PAN was explored by Raman (Fig. 9) and XPS (Fig. 10). As shown in Fig. 9, the major changes are observed in the region from 1200 to 1700 $cm^{-1}$. The strong absorption peak at 1596 $cm^{-1}$ corresponds to the C=C stretching vibration of the quinonoid ring, and the bands at 1565 and 1490 $cm^{-1}$ correspond to C—C stretching vibration of the quinonoid ring and C=N stretching vibrations in quinonoid units, respectively. The high intensity in the region of 1345 $cm^{-1}$ corresponds to $C \sim N^+$ vibrations which are characteristic of PANI salt [39,40]. After treated with Cr(VI) solution, the peaks at 1596 $cm^{-1}$ have shifted to 1584 $cm^{-1}$, indicating a stronger interaction between PANI and Cr(VI) absorbed. Moreover, the peaks at 1596 and 1490 $cm^{-1}$ become stronger and the intensity of the band at about 1345 $cm^{-1}$ decreased after treatment with Cr (VI). These results indicated that the PANI has been oxidized from its protonated emeraldine state to pernigraniline state by Cr(VI).

XPS was employed to investigate the Cr element chemical state (Fig. 10). As documented, for the Cr2p XPS spectrum, the characteristic binding energy peaks at 577.0–580.0 eV and 586.0–588.0 eV correspond to Cr(III), and the peaks at 580.0–580.5 eV and 589.0–590.0 eV attributable to Cr(VI) [41]. Fig. 10(a) shows the Cr2p XPS spectrum of the PANI/PAN composites treated with Cr(VI) solution. The binding energy peaks of Cr2p were observed at 578.1 and 586.8 eV, indicating that the adsorbed Cr is

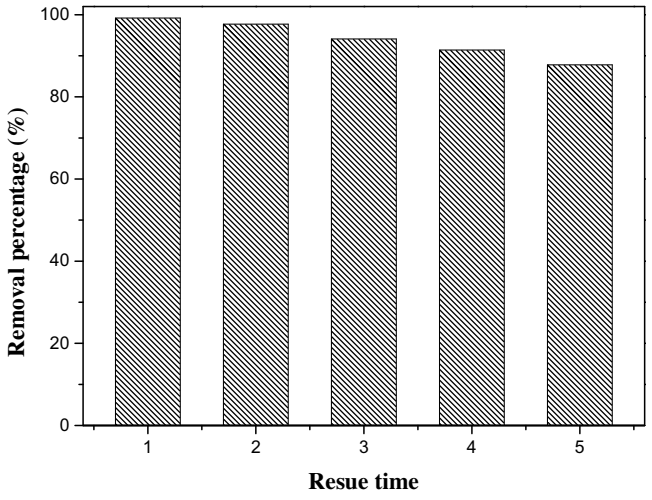


**Fig. 11.** Cr(VI) removal efficiency of the regenerated PANI/PAN. (Cr(VI): 5.0 mg/L, PANI/PAN: 10 mg, pH: 1.0, treating time: 6 h).

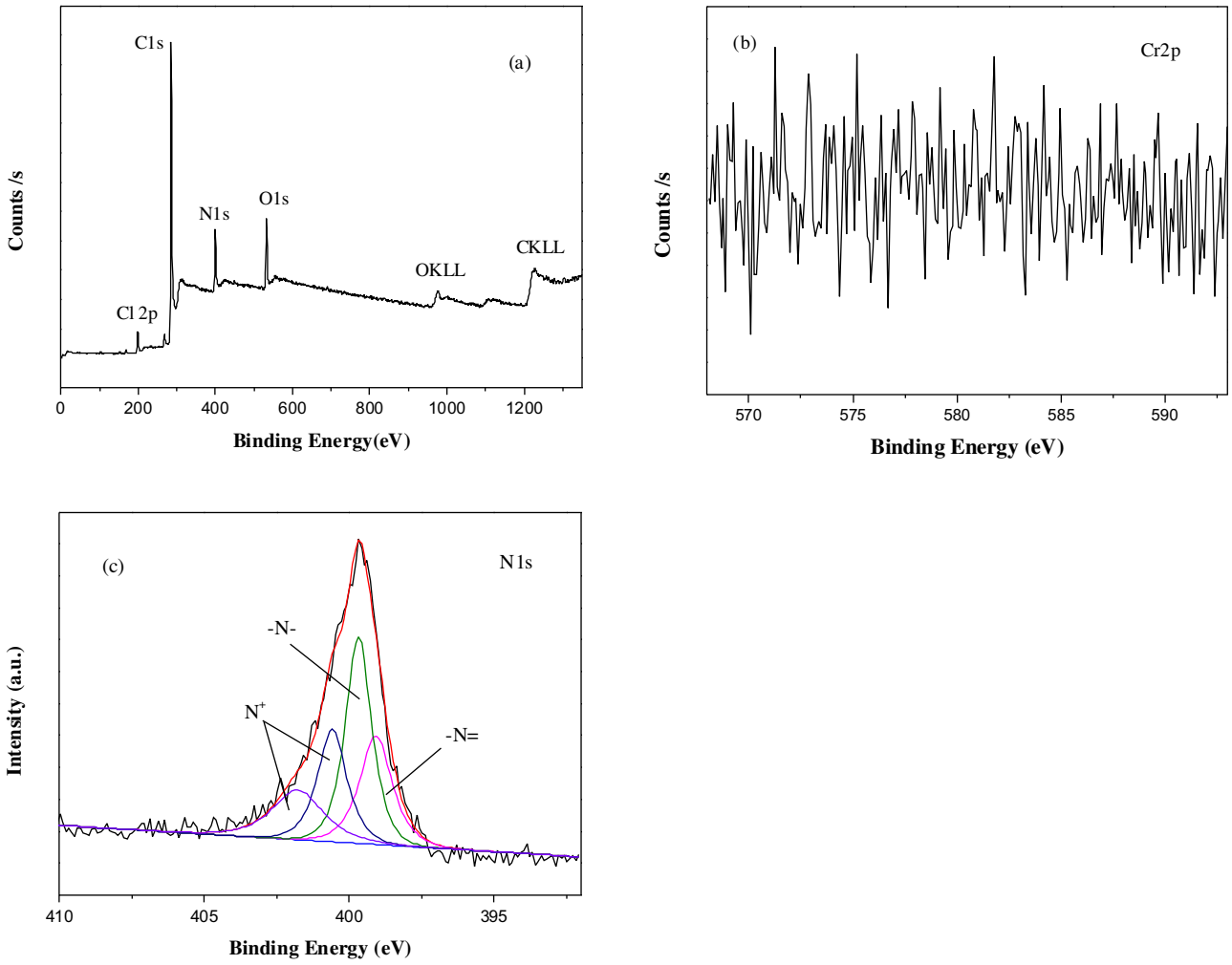


**Fig. 12.** XPS wide scan (a), Cr2p (b) and N1s (c) spectra of 0.1 M HCl regenerated PANI/PAN.

in the form of Cr(III). And the peaks have shifted slightly compared with the literature reports [41]. No Cr(VI) was detected on the PANI/PAN by the Cr2p XPS spectra. The result suggested that all Cr (VI) adsorbed on the surface of PANI/PAN was reduced to Cr(III). The N1 s spectrum can be fitted into three major peak components with binding energy at 398.6, 399.2 and 400.6 eV (Fig. 10(b)), which are attributed to the imine group (-N = ), amine group (-NH-) and protonated nitrogen ($N^+$), respectively [31]. The ratio of amine groups (-NH-) decreased from 57.8 mol% to 19.2 mol% after adsorption of Cr(VI). However, the ratio of imine groups (-N = ) increased from 11.3 mol% to 65.3 mol%. The results indicate that PANI has been oxidized after treatment with Cr(VI) solution [42]. Generally, the Cr(VI) adsorbed on the PANI/PAN was reduced to Cr (III) by amine groups, leading to the transformation of PANI from its protonated emeraldine state to pernigraniline state [42].

*3.2.8. Regeneration study*

For practical application, the recycling and regeneration of the adsorbent is indispensable. The PAN fibers mat can be easily recycled due to its large size. A sample of the PANI/PAN already treated with Cr(VI) solution was used for the regeneration study. The Cr was desorbed from Cr(VI)-adsorbed PANI/PAN by 0.1 M HCl solution at room temperature. The regenerated PANI/PAN were used to treat 5.0 mg/L Cr(VI) solution (25 mL) for 6 h. The adsorption–desorption was conducted for 5 cycles, and the Cr (VI) removal efficiency was measured. As shown in Fig. 11, the PANI/PAN fibers mat showed good reuse performance. The removal efficiency still remained 87.84% after 5 cycles.

To better understand the regeneration process the Raman (Fig. 9) and XPS was employed (Fig. 12). As is shown in Fig. 9(b) and (c), the peaks at 1584 $cm^{-1}$ have shifted to 1596 $cm^{-1}$ after regenerated by 0.1 M HCl solution. Moreover, the band at 1345 $cm^{-1}$ relatively increased, and the bands at about 1596 and 1490 $cm^{-1}$ decreased. The results indicate that PANI has been reduced by 0.1 M HCl. In the XPS wide scan spectra of the regenerated PANI/PAN (Fig. 12a), Cl2p signals appeared at 196.9 eV, meanwhile S2p signals disappeared, which reveals that PANI was redoped by HCl. And the results indicate that Cr(III) has been dedoped by HCl. AS is shown in Fig. 12(a) and (b), almost no Cr was detected on the PANI/PAN after regenerated by 0.1 M HCl. Deconvolution of N1 s spectrum of regenerated PANI/PAN is shown in Fig. 12(c), in which N1 s can be deconvoluted into four peaks [31] centered at 399.1(-N = ), 399.7(-NH-), 400.6(=N + ) and 401.8(-N + ) with area fractions of 19.3, 29.5, 18 and 13.9, respectively. Compared to Fig. 10(b), the ratio of —N- increased and the ratio of —N = decreased after regeneration. The results indicate that the pernigraniline of PANI can be reduced to emeraldine salt in acidic solution [17].

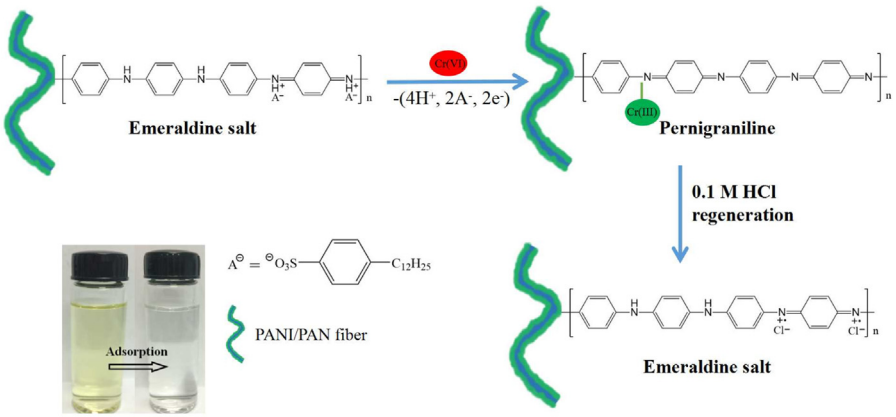


**Fig. 13.** Proposed pathway of Cr(VI) removal by PANI/PAN fibers mat.

These regeneration phenomenons of PANI from PB to EB salt in acidic aqueous solution quite conforms to the previous reports that the PB form of PANI is unstable under ambient conditions [17,39]. Especially, MacDiarmid et al. [39] proved that the PANI can be reduced from its pernigraniline form to emeraldine oxidation state by 1 M HCl with concomitant ring chlorination. In addition, Qiu et al. [40] proved that the PANI regenerated by 0.1 M HCl have a good thermal stability. Based on the above studies, we think that the proposed mechanism of adsorption and regeneration in this study can be shown as Fig. 13. The Cr(VI) is initially adsorbed on the surface of the PANI/PAN, and followed by the reduction of Cr(VI) to Cr(III) by the amine functional groups of PANI. And the treatment of pernigraniline with HCl solution resulted in its reduction to the emeraldine oxidation state with concomitant ring chlorination [17].

## 4. Conclusion

Solution-blowing technique was used to fabricate PAN nanofibers mat. The fiber diameter of PAN nanofibers mat ranged from 348 to 612 nm by altering the spinning processing parameters. Then the PANI/PAN core/shell nanofibers mat were fabricated by polymerizing PANI on PAN template. By regulating the molar ratio of oxidant to monomer, the morphological evolution of the composite fiber mat could be controlled. The PANI/PAN fibers mat presented a great performance for Cr(VI) adsorption. From the XPS and Raman analysis, reduction was the main mechanism for Cr(VI) removal. The Cr(VI) adsorption by PANI/PAN was highly dependent on the initial solution pH and had a higher adsorption capacity at pH = 1.0. These PANI/PAN adsorbents (10 mg) were able to remove 5 mg/L Cr(VI) solution (25 mL) within 300 min. The Cr(VI) removal percentage decreased with increasing the initial Cr(VI) concentration. The adsorption kinetic was fitted better with pseudo-second-order. Isotherm data were in good accordance with the Langmuir isotherm model. Thermodynamic study suggested that the adsorption process is spontaneous, endothermic and marked with an increase in randomness at the solid–liquid interface. The regenerated PANI/PAN by 0.1 M HCl solution exhibited a fairly good performance of Cr(VI) removal, indicating that PANI/PAN are promising adsorbents for effective Cr(VI) removal.

## Acknowledgements

This work was supported by the National Natural Science Foundation of China (Grant No.51573135 and 51307169), the Key Project in Application of Basic and Frontier project of Tianjin Municipal (Grant No. 13JCZDJC32100) and Tianjin Research Program of Application Foundation and Advanced Technology (No.16JCYBJC17100).

## References

[1] V. Gupta, S. Agarwal, T.A. Saleh, Chromium removal by combining the magnetic properties of iron oxide with adsorption properties of carbon nanotubes, Water Res. 45 (2011) 2207–2212.
[2] C. Xu, B. Qiu, H. Gu, X. Yang, H. Wei, X. Huang, Y. Wang, D. Rutman, D. Cao, S. Bhana, Synergistic interactions between activated carbon fabrics and toxic hexavalent chromium, ECS J. Solid State Sci. Technol. 3 (2014) M1–M9.
[3] Z. Modrzejewska, W. Kaminski, Separation of Cr(VI) on chitosan membranes, Ind. Eng. Chem. Res. 38 (1999) 4946–4950.
[4] A. Qian, P. Liao, S. Yuan, M. Luo, Efficient reduction of Cr(VI) in groundwater by a hybrid electro-Pd process, Water Res. 48 (2014) 326–334.
[5] S. Rengaraj, C.K. Joo, Y. Kim, J. Yi, Kinetics of removal of chromium from water and electronic process wastewater by ion exchange resins: 1200H, 1500H and IRN97H, J. Hazard. Mater. 102 (2003) 257–275.
[6] L.C. Hsu, S.L. Wang, Y.C. Lin, M.K. Wang, P.N. Chiang, J.C. Liu, W.H. Kuan, C.C. Chen, Y.M. Tzou, Cr(VI) removal on fungal biomass of Neurospora crassa: the importance of dissolved organic carbons derived from the biomass to Cr(VI) reduction, Environ. Sci. Technol. 44 (2010) 6202–6208.
[7] R. Zhang, B. Wang, H. Ma, Studies on Chromium (VI) adsorption on sulfonated lignite, Desalination 255 (2010) 61–66.
[8] Y. Wu, X. Ma, M. Feng, M. Liu, Behavior of chromium and arsenic on activated carbon, J. Hazard. Mater. 159 (2008) 380–384.
[9] M. Dakiky, M. Khamis, A. Manassra, M. Mer'eb, Selective adsorption of chromium(VI) in industrial wastewater using low-cost abundantly available adsorbents, Adv. Environ. Res. 6 (2002) 533–540.
[10] D. Zhang, S. Wei, C. Kaila, X. Su, J. Wu, A.B. Karki, D.P. Young, Z. Guo, Carbon-stabilized iron nanoparticles for environmental remediation, Nanoscale 2 (2010) 917–919.
[11] H. Gu, S.B. Rapole, J. Sharma, Y. Huang, D. Cao, H.A. Colorado, Z. Luo, N. Haldolaarachchige, D.P. Young, B. Walters, S. Wei, Z. Guo, Magnetic polyaniline nanocomposites toward toxic hexavalent chromium removal, RSC Adv. 2 (2012) 11007–11018.
[12] A. Olad, R. Nabavi, Application of polyaniline for the reduction of toxic Cr(VI) in water, J. Hazard. Mater. 147 (2007) 845–851.
[13] A.G. Yavuz, E. Dincturk-Atalay, A. Uygun, F. Gode, E. Aslan, A comparison study of adsorption of Cr(VI) from aqueous solutions onto alkyl-substituted polyaniline/chitosan composites, Desalination 279 (2011) 325–331.
[14] J.Y. Shimano, A.G. MacDiarmid, Polyaniline, a dynamic block copolymer: key to attaining its intrinsic conductivity? Synth. Met. 123 (2001) 251–262.
[15] Z. Rozlívková, M. Trchová, I. Šeděnková, M. Špírková, J. Stejskal, Structure and stability of thin polyaniline films deposited in situ on silicon and gold during precipitation and dispersion polymerization of aniline hydrochloride, Thin Solid Films 519 (2011) 5933–5941.
[16] P.A. Kumar, S. Chakraborty, M. Ray, Removal and recovery of chromium from wastewater using short chain polyaniline synthesized on jute fiber, Chem. Eng. J. 141 (2008) 130–140.
[17] X. Guo, G.T. Fei, H. Su, L. De Zhang, High-performance and reproducible polyaniline nanowire/tubes for removal of Cr(VI) in aqueous solution, J. Phys. Chem. C 115 (2011) 1608–1613.
[18] J. Huang, R.B. Kaner, The intrinsic nanofibrillar morphology of polyaniline, Chem. Commun. (2006) 367–376, doi:http://dx.doi.org/10.1039/b510956f.

[19] N.R. Chiou, A.J. Epstein, Polyaniline nanofibers prepared by dilute polymerization, Adv. Mater. 17 (2005) 1679–1683.
[20] X. Zhang, J. Zhu, N. Haldolaarachchige, J. Ryu, D.P. Young, S. Wei, Z. Guo, Synthetic process engineered polyaniline nanostructures with tunable morphology and physical properties, Polymer 53 (2012) 2109–2120.
[21] S. Nasreen, S. Sundarrajan, S. Nizar, R. Balamurugan, S. Ramakrishna, Advancement in electrospun nanofibrous membranes modification and their application in water treatment, Membranes 3 (2013) 266.
[22] K. Saeed, S. Haider, T.-J. Oh, S.-Y. Park, Preparation of amidoxime-modified polyacrylonitrile (PAN-oxime) nanofibers and their applications to metal ions adsorption, J. Membr. Sci. 322 (2008) 400–405.
[23] J. Wang, K. Pan, Q. He, B. Cao, Polyacrylonitrile/polypyrrole core/shell nanofiber mat for the removal of hexavalent chromium from aqueous solution, J. Hazard. Mater. 244–245 (2013) 121–129.
[24] E.S. Medeiros, G.M. Glenn, A.P. Klamczynski, W.J. Orts, L.H.C. Mattoso, Solution blow spinning: a new method to produce micro- and nanofibers from polymer solutions, J. Appl. Polym. Sci. 113 (2009) 2322–2330.
[25] L. Zhang, P. Kopperstad, M. West, N. Hedin, H. Fong, Generation of polymer ultrafine fibers through solution (air-) blowing, J. Appl. Polym. Sci. 114 (2009) 3479–3486.
[26] M.R. Unnithan, T.S. Anirudhan, The kinetics and thermodynamics of sorption of chromium(VI) onto the Iron(III) complex of a carboxylated polyacrylamide-grafted sawdust, Ind. Eng. Chem. Res. 40 (2001) 2693–2701.
[27] Y. Zhou, X. Hu, M. Zhang, X. Zhuo, J. Niu, Preparation and characterization of modified cellulose for adsorption of Cd(II), Hg(II), and acid fuchsin from aqueous solutions, Ind. Eng. Chem. Res. 52 (2013) 876–884.
[28] P.A. Kumar, S. Chakraborty, Fixed-bed column study for hexavalent chromium removal and recovery by short-chain polyaniline synthesized on jute fiber, J. Hazard. Mater. 162 (2009) 1086–1098.
[29] J.A. Marins, B.G. Soares, K. Dahmouche, S.J.L. Ribeiro, H. Barud, D. Bonemer, Structure and properties of conducting bacterial cellulose-polyaniline nanocomposites, Cellulose 18 (2011) 1285–1294.
[30] G. Ćirić-Marjanović, M. Trchová, J. Stejskal, The chemical oxidative polymerization of aniline in water: Raman spectroscopy, J. Raman Spectrosc. 39 (2008) 1375–1387.
[31] E.T. Kang, K.G. Neoh, K.L. Tan, Polyaniline A polymer with many interesting intrinsic redox states, Prog. Polym. Sci. 23 (1998) 277–324.
[32] H. Zhou, Z. Shi, Y. Lu, Conducting polyaniline/poly(tetrafluoroethylene) composite films with tunable surface morphology and hydrophilicity, Synth. Met. 160 (2010) 1925–1930.
[33] X.-F. Sun, Y. Ma, X.-W. Liu, S.-G. Wang, B.-Y. Gao, X.-M. Li, Sorption and detoxification of chromium(VI) by aerobic granules functionalized with polyethylenimine, Water Res. 44 (2010) 2517–2524.
[34] N. Mohammadi, H. Khani, V.K. Gupta, E. Amereh, S. Agarwal, Adsorption process of methyl orange dye onto mesoporous carbon material–kinetic and thermodynamic studies, J. Colloid Interface Sci. 362 (2011) 457–462.
[35] Y. Zheng, W. Wang, D. Huang, A. Wang, Kapok fiber oriented-polyaniline nanofibers for efficient Cr(VI) removal, Chem. Eng. J. 191 (2012) 154–161.
[36] A. Mirmohseni, A. Oladegaragoze, Detection and determination of CrVI in solution using polyaniline modified quartz crystal electrode, J. Appl. Polym. Sci. 85 (2002) 2772–2780.
[37] T. Aman, A.A. Kazi, M.U. Sabri, Q. Bano, Potato peels as solid waste for the removal of heavy metal copper(II) from waste water/industrial effluent, Colloid Surf. B 63 (2008) 116–121.
[38] Y. Jiang, H. Pang, B. Liao, Removal of copper(II) ions from aqueous solution by modified bagasse, J. Hazard. Mater. 164 (2009) 1–9.
[39] A.G. MacDiarmid, S.K. Manohar, J.G. Masters, Y. Sun, H. Weiss, A.J. Epstein, Polyaniline Synthesis and properties of pernigraniline base, Synth. Met. 41 (1991) 621–626.
[40] B. Qiu, C. Xu, D. Sun, H. Wei, X. Zhang, J. Guo, Q. Wang, D. Rutman, Z. Guo, S. Wei, Polyaniline coating on carbon fiber fabrics for improved hexavalent chromium fx1removal, RSC Adv. 4 (2014) 29855–29865.
[41] D. fx7[41], Y.-S. Park, J.M. Yun, X.A.S. Park, X.P.S. studies, on chromium-binding groups of biomaterial during Cr(VI) biosorption, J. Colloid Interface Sci. 317 (2008) 54–61.
[42] Y. Chen, E.T. Kang, K.G. Neoh, S.L. Lim, Z.H. Ma, K.L. Tan, Intrinsic redox states of polyaniline studied by high-resolution X-ray photoelectron spectroscopy, Colloid Polym. Sci. 279 (2001) 73–76.